The RoadMapping Code: How to deal with "Real World" Issues in Action-based Dynamical Modelling the Milky Way

W. Trick[1,2], J. Bovy[3,4], and H.-W. Rix[1]

trick@mpia.de

Subject headings: Galaxy: disk — Galaxy: fundamental parameters — Galaxy: kinematics and dynamics — Galaxy: structure

Contents

1. Dynamical Modelling

[1]Max-Planck-Institut für Astronomie, Königstuhl 17, D-69117 Heidelberg, Germany

[2]Correspondence should be addressed to trick@mpia.de.

[3]Institute for Advanced Study, Einstein Drive, Princeton, NJ 08540, USA

[4]Hubble fellow

1.1. Model

1.1.1. Actions

[TO DO]

1.1.2. Potential models

[TO DO] Mention different ways to calculate actions in different potentials.

1.1.3. Distribution function

The structure of the MW disk is still under debate: While many still support the thin-thick disk dichotomy in the MW disk (references ???), Bovy et al. (2012b) found indications that the MW disk might actually be a super-position of many stellar sub-popluations with a continuous spectrum of scale heights, scale lengths, metallicity and [α/Fe] abundances (dubbed mono-abundance populations (*MAP*s)). Further investigation lead to the findings that *MAP*s in the MW disk have a simple spatial structure that follows an exponential in both radial and vertical direction (Bovy et al. 2012d). The corresponding velocity dispersion profile of the *MAP*s also decreases exponentially with radius and is nearly independent of height above the plane, i.e. quasi-isothermal (Bovy et al. 2012c). The radial decrease in vertical velocity dispersion has, according to Bovy et al. (2012c), a long scale length of $h_{\sigma,z} \sim 7$ kpc for all *MAP*s . Older *MAP*s , which are characterized by lower metallicities and [α/Fe] abundances, have in general shorter density scale lengths, larger scale heights and velocity dispersion (Bovy et al. 2012d). Ting et al. (2013) and Bovy & Rix (2013) finally proposed that these findings could be employed for dynamical modelling techniques using

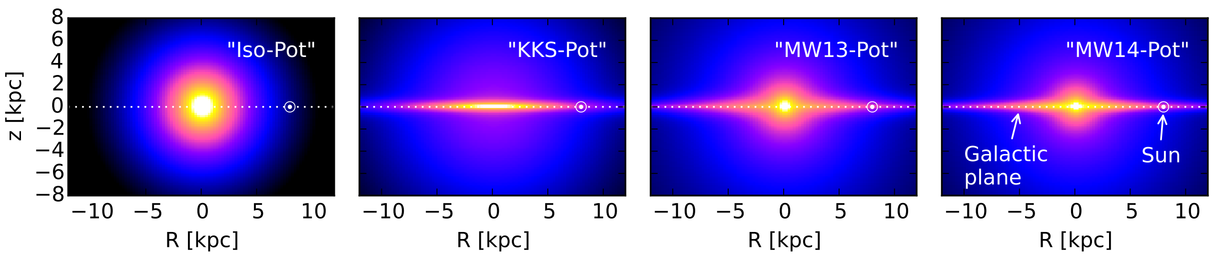

Fig. 1.— [TO DO]

Table 1. Caption [TO DO].

name	potential type	free parameters p_Φ		action calculation	reference
"Iso-Pot"	isochrone potential	circular velocity at the sun isochrone scale length	$v_{\mathrm{circ}} = 230$ km s^{-1} $b = 0.9$ kpc	***analytical and exact*** J_r, J_ϑ, L_z; use $J_r \rightarrow J_R, J_\vartheta \rightarrow J_z$ in eq. (???)	Binney & Tremaine (2008)
"KKS-Pot"	2-component Kuzmin-Kutuzov- Stäckel potential	circular velocity at the sun focal distance of coordinate system[a] axis ratio of the coordinate surfaces[a] ... ...of the disk component ...of the halo component relative contribution of the disk mass to the total mass	$v_{\mathrm{circ}} = 230$ km s^{-1} $\Delta = 0.3$ $\left(\frac{a}{c}\right)_{\mathrm{Disk}} = 20$ $\left(\frac{a}{c}\right)_{\mathrm{Halo}} = 1.07$ $k = 0.28$	***exact*** J_R, J_z, L_z using "Stäckel Fudge" (Binney 2012) and interpolation on action grid (**?**)	Batsleer & Dejonghe (1994)
"MW13-Pot"	MW-like potential with fixed Hernquist bulge, 2 exponential disks (stars + gas), spherical power-law halo	circular velocity at the sun stellar disk scale length stellar disk scale height relative halo contribution to $v^2_{\mathrm{circ}}(R_\odot)$ "flatness" of rotation curve	$v_{\mathrm{circ}} = 230$ km s^{-1} $R_d = 3$ kpc $z_h = 0.4$ kpc $f_h = 0.5$ $\frac{\mathrm{d}\ln(v_{\mathrm{circ}}(R_\odot))}{\mathrm{d}\ln(R)} = 0$	***approximate*** J_R, J_z, L_z using "Stäckel Fudge" (Binney 2012) and interpolation on action grid (**?**)	Bovy & Rix (2013)
"MW14-Pot"	MW-like potential with cutoff power-law bulge, Miyamoto-Nagai stellar disk, NFW halo	-	-	see "MW13-Pot"	**?**

[a]The coordinate system of each of the two Stäckel-potential components is $\frac{R^2}{\tau_{i,p}+\alpha_p} + \frac{z^2}{\tau_{i,p}+\gamma_p} = 1$ with $p \in \{\mathrm{Disk}, /\mathrm{Halo}\}$ and $\tau_{i,p} \in \{\lambda_p, \nu_p\}$. Both components have the same focal distance $\Delta = \sqrt{\gamma_p - \alpha_p}$, to make sure that the superposition of the two components itself is still a Stäckel potential. The axis ratio of the coordinate surfaces $\left(\frac{a}{c}\right)_p := \sqrt{\frac{\alpha_p}{\gamma_p}}$ describes the flattness of the corresponding Stäckel component.

action-based distribution functions. An action-based distribution function, that is flexible enough to describe the spectrum of simple phase-space distributions of different *MAP*s , is the quasi-isothermal distribution function (qDF) by Binney & McMillan (2011), as demonstrated by Ting et al. (2013). The qDF by Binney & McMillan (2011) is a function of the actions $\boldsymbol{J} = (J_R, J_z, L_z)$ and has the form

$$
\begin{aligned}
\mathrm{qDF}(\boldsymbol{J} \mid p_{\mathrm{DF}}) &= f_{\sigma_R}(J_R, L_z \mid p_{\mathrm{DF}}) \times f_{\sigma_z}(J_z, L_z \mid p_{\mathrm{DF}}) \\
\text{with } f_{\sigma_R}(J_R, L_z \mid p_{\mathrm{DF}}) &= n \times \frac{\Omega}{\pi \sigma_R^2(R_g)\kappa} \left[1 + \tanh\left(L_z/L_0\right)\right] \exp\left(-\frac{\kappa J_R}{\sigma_R^2(R_g)}\right) \\
f_{\sigma_z}(J_z, L_z \mid p_{\mathrm{DF}}) &= \frac{\nu}{2\pi \sigma_z^2(R_g)} \exp\left(-\frac{\nu J_z}{\sigma_z^2(R_g)}\right)
\end{aligned}
$$

Here $R_g \equiv R_g(L_z)$ and $\Omega \equiv \Omega(L_z)$ are the (guidig-center) radius and the circular frequency of the circular orbit with angular momentum L_z in a given potential. $\kappa \equiv \kappa(L_z)$ and $\nu \equiv \nu(L_z)$ are the radial/epicycle (κ) and vertical (ν) frequencies with which the star would oscillate around the circular orbit in R- and z-direction when slightly perturbed (Binney & Tremaine 2008). The term $[1 + \tanh(L_z/L_0)]$ suppresses counter-rotation for orbits in the disk with $L \gg L_0$ which we set to a random small value ($L_0 = 10 \times R_\odot/8 \times v_{\mathrm{circ}}(R_\odot)/220$).
For this qDF to be able to incorporate the findings by Bovy et al. 2012 about the phase-space structure of *MAP*s summarized above, we set the functions n, σ_R and σ_z, which indirectly set the stellar number density and radial and vertical velocity dispersion profiles,

$$
\begin{aligned}
n(R_g) &\propto \exp\left(-\frac{R_g}{h_R}\right) \\
\sigma_R(R_g) &= \sigma_{R,0} \times \exp\left(-\frac{R_g - R_\odot}{h_{\sigma_R}}\right) \\
\sigma_z(R_g) &= \sigma_{z,0} \times \exp\left(-\frac{R_g - R_\odot}{h_{\sigma_z}}\right).
\end{aligned}
$$

The qDF for each *MAP* has therefore a set of five free parameters p_{DF}: the density scale length of the tracers h_R, the radial and vertical velocity dispersion at the solar position $R_\odot$, $\sigma_R, 0$ and $\sigma_z, 0$, and the scale lengths h_{σ_R} and h_{σ_z}, that describe the radial decrease of the velocity dispersion. The *MAP*s we use for illustration through out this work are summarized in table ???.

[TO DO] [To Do here: Also mention how the density is calculated.]

1.1.4. Selection function: observed volume and completeness

[TO DO]

Table 2. Caption [TO DO]. The parameters of the "cooler" ("hotter") *MAP*s were chosen such, that the they have the same σ_R/σ_z ratio as the "hot" ("cool") *MAP* . Hotter populations have shorter tracer scale lengths (Bovy et al. 2012d) and the velocity dispersion scale lengths were fixed according to Bovy et al. (2012c).

name of *MAP*	free parameters p_{DF}				
	h_R [kpc]	σ_R [km s^{-1}]	σ_z [km s^{-1}]	h_{σ_R} [kpc]	h_{σ_z} [kpc]
"hot"	2	55	66	8	7
"cool"	3.5	42	32	8	7
"cooler"	2 +50%	55-50%	66-50%	8	7
"hotter"	3.5-50%	42+50%	32+50%	8	7

2. Results

2.1. What if our assumed distribution function differs from the stars' DF?

Sanders & Binney (2015) and ??? develop extended distribution functions (EDFs), that extend action-based DFs to also describe the distribution of the star's metallicities. While a full chemo-dynamical modelling, including metallicity as well as α- and other chemical abundances, is ultimately the right way to go, the form of the EDFs still depends on a lot of additional assumptions. By looking at fig. 6 in Bovy & Rix (2013) (other references???) we doubt that a final version of an EDF will have a simple form in action-metallicity space. Motivated by the findings by Bovy et al. 2012, we therefore resign to the simpler approach outlined in Bovy & Rix (2013) and here, were metallicity and α-abundances are implicitly taken into account by describing each MAP separately by one qDF. This procedure could have two caveats:
First, the binning of the stars according to their abundances could lead to pollution of one MAP, by either choosing the bin sizes too large, or too small compared to the stars' inherent abundance errors.
Second, while Ting et al. (2013) makes us confident that the qDF is indeed a good functional form to describe each MAP, it could very well be, that the stars' true distribution is close to but not exactly of the family of assumed qDFs.
We try to investigate both this issues with the following test: We draw two mock data sets, each from a different qDF, and mix the stars in different fractions together. We then analyse this mixture by assuming all stars sill came from a single qDF. The results are shown in fig. 3 and 4.
In example 1 and 2 (fig. 3) we consider two very different MAPs, a hotter and a cooler one, that are mixed together in different fractions. This test could be understood as the true distribution of stars being a linear combination of two very different qDFs and we investigate how this deviation from a single qDF affects the potential recovery. We find that for a MAP that follows approximately a hot population (polluted by up to $\sim$ 30% of cooler stars), the potential can still be very well recovered. The analysis of cooler MAPs are much more affected by pollution due to hotter MAP stars.
In example 3 and 4 (fig. 4) it is investigated how different the qDF parameters of two MAPs are allowed to be to be still able to constrain the true potential. This test could be seen as a model scenario for decreasing bin sizes in the metallicity-α plane when sorting stars in different MAPs, assuming that there is a smooth variation of qDF within the metallicity-α plane. We find that differences of 20% in the qDF parameters of two neighbouring MAPs can still give quite good constraints on the potential parameters. We compare this with the relative difference in the qDF parameters in the bins in fig. 6 of Bovy & Rix (2013), which have sizes of $[Fe/H] = 0.1$ dex and $\Delta[\alpha/Fe] = 0.05$ dex. It seems that these bin sizes are large enough to make sure that $\sigma_{R,0}$ and $\sigma_{z,0}$ of neighbouring MAPs do not differ more than

20%. As fig. 3 and 4 suggests especially the tracer scale length h_R needs to be recovered to get the potential right. For this parameter however the bin sizes in fig. 6 of Bovy & Rix (2013) might not yet be small enough to ensure no more than 20% of difference in neighbouring h_R, especially in the low-α ($[\alpha/Fe] \lesssim 0.2$), intermediate-metallicity ($[Fe/H] \sim -0.5$) MAPs.

[TO DO: think, if this might better be two different sections. ???? one for MixDiff about neighbouring MAPS and one for MixCont for difference in DF. ????]

Collection of possible tests and plots

- *Test 1:* Vary the fraction of pollution. Idea behind this: What if the stellar distribution has a different shape, e.g. added "wings", or had a different tracer density decrease with R. Would be however great, if we could show how the mixture of qdf's quanlitatively changes the shape of the df. Any ideas?
  Plot 1: Violin plot: x-axis - fraction of pollution. y-axis: b-parameter and one or two qdf parameters.

- *Test 2:* same as Test 1, but this time vary the degree of difference and make it 50% pollution. Idea behind this: What happens, if we have errors in the abundances and mix different MAPs? For this it would be could to compare how much the qdf parameters of neighbouring MAPs differ and how big the difference between MAPs can be, such that it still can reproduce the potential.
  Plot 2: Violin plot: x-axis - difference in qdf parameters. y-axis: b-parameter and one or two qdf parameters.

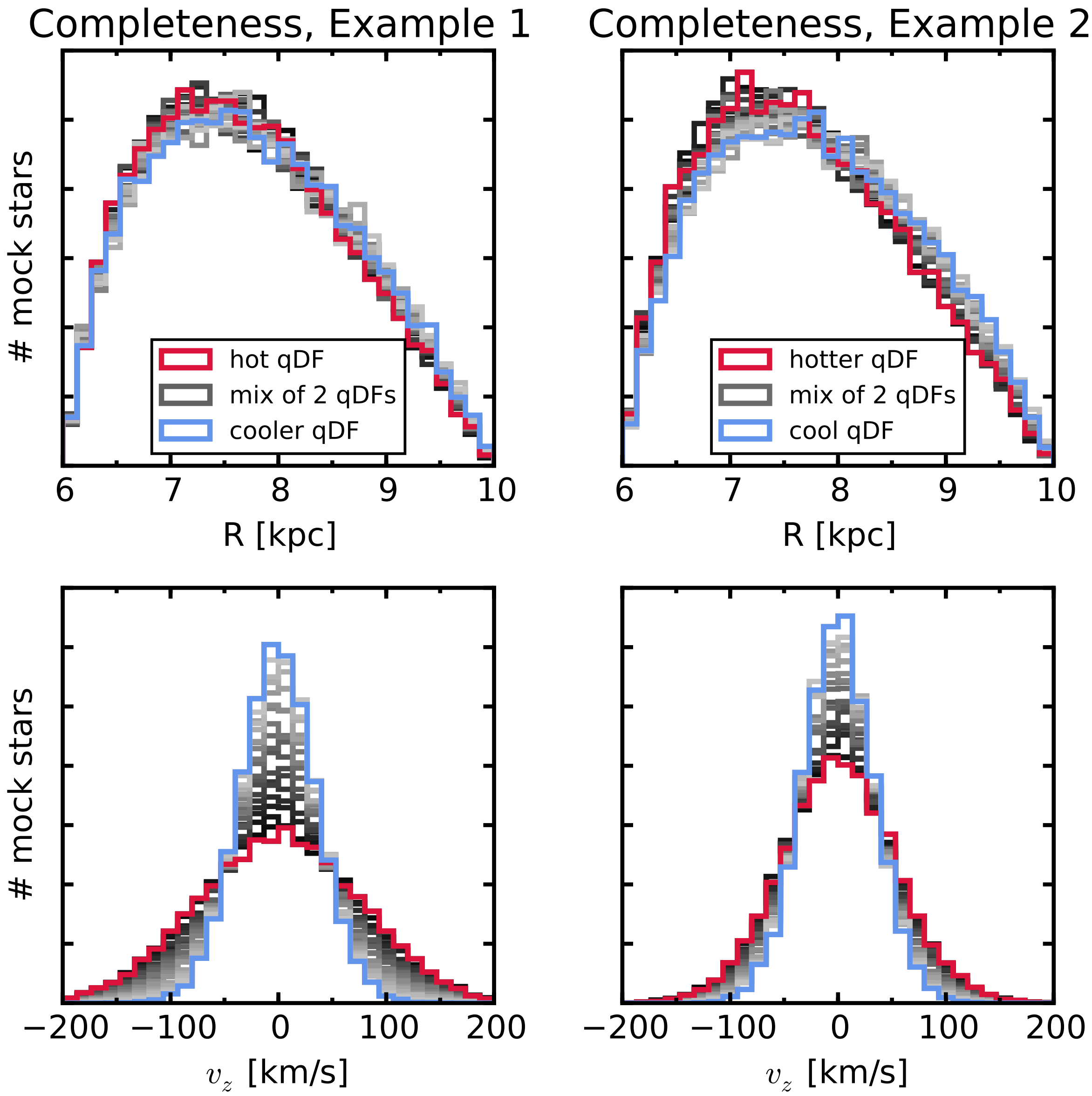

Fig. 2.— Distribution of mock data in two coordinates (R and v_z), created by mixing different amounts of stars drawn from two different qDFs. The red and blue histograms show data sets drawn from a single qDF only: the "hot" and the "cooler" *MAP*s (Example 1) in the left panels, and the "cool" and "hotter" *MAP*s (Example 2) in the right panels (see table 2). The gray histograms show data drawn from a superpositions of two qDFs. In total there are always 20,000 stars in the data set. The color coding represents the different mixing rates (black - all hot, bright gray - all cool) and is the same as in figure 3, where the corresponding modelling results for each data set are shown. This demonstrates how mixing two qDFs can be used as a test case for adding or removing wings to a pure qDF.

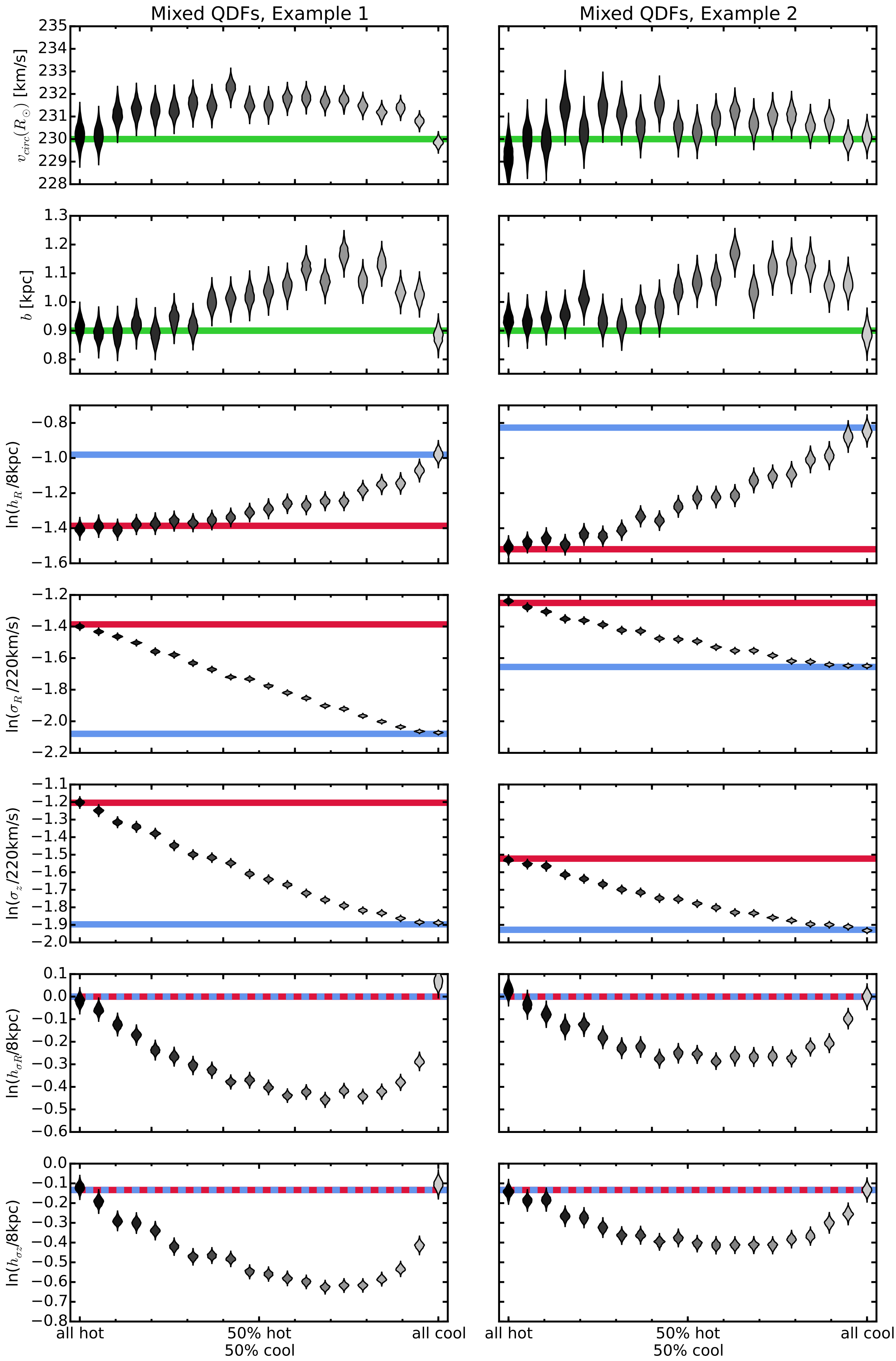

Fig. 3.— (Caption on next page.)

Fig. 3.— (Continued.) The dependence of the parameter recovery on degree of pollution and 'hotness' of the stellar population. To model the pollution of a hot stellar population by stars coming from a cool population and vice versa, we mix varying amounts of stars from two very different populations, as indicated on the x-axis. (The corresponding mock data sets are shown, in the same gray scales, in fig. 2.) Both populations come from same potential, the isochrone potential "Iso-Pot" from table 1 (true potential parameters are indicated by green lines). The composite data set is then fit with one single qDF. Example 1 (left) mixes the "hot" *MAP* with the "cooler" *MAP* in table 2, while example 2 (right) mixes the "cool" *MAP* with the "hotter" *MAP* . True parameters of the hotter of the two populations are shown as red lines, those of the cooler populations as blue lines. The violines represent the marginalized likelihoods found from the MCMC analysis. [TO DO: This was done using the current qDF to set the fitting range. Nvelocity=24 and Nsigma=5 is high enough (though not perfect). Maybe redo with fiducial qDF to be consistent with MixDiff test. ???]

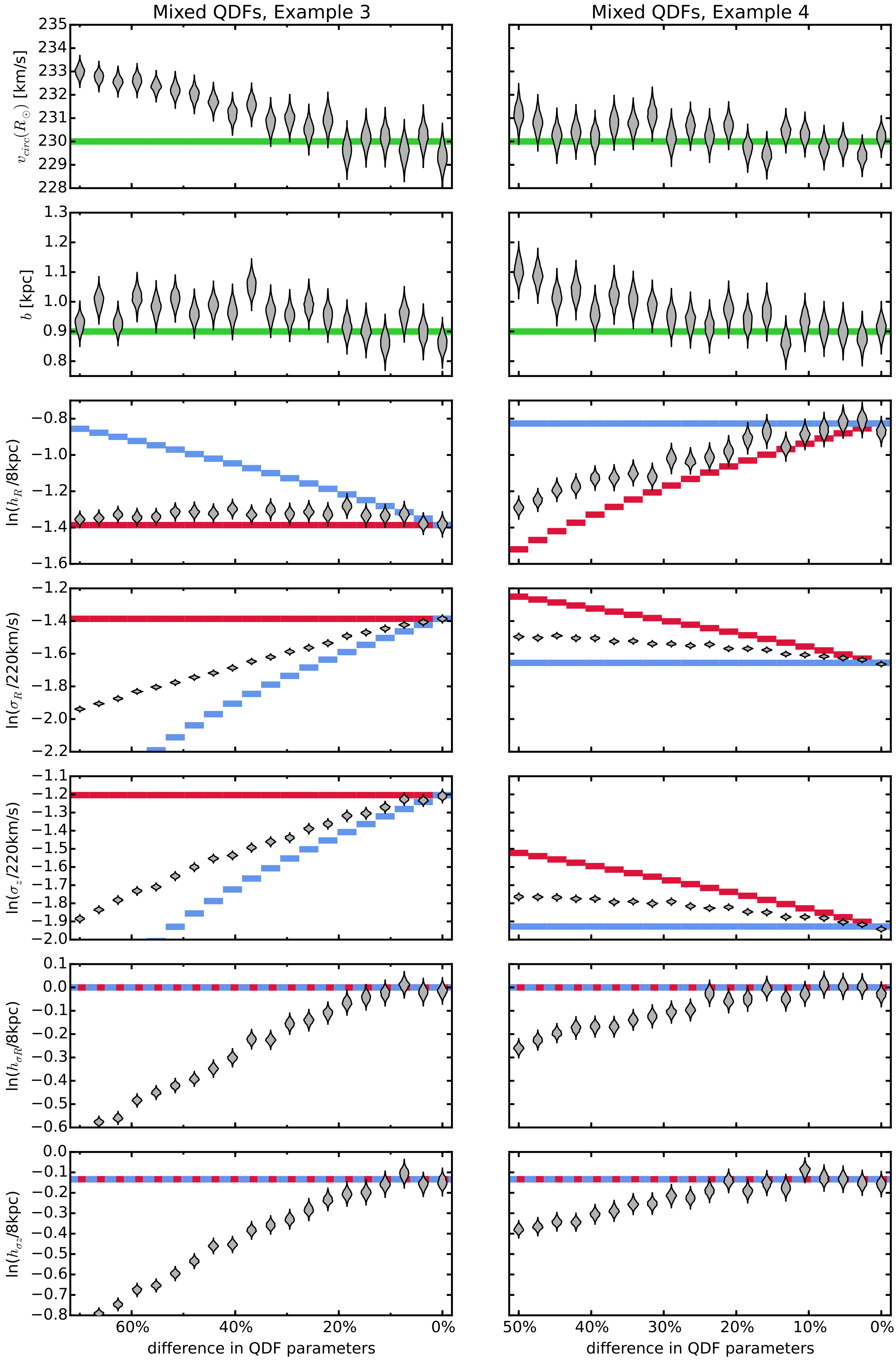

Fig. 4.— (Caption on next page.)

Fig. 4.— (Continued.) The dependence of the parameter recovery on the difference in DF parameters of the mixture of two stellar populations and their 'hotness'. [TO DO], Maybe different/same x-axis??? [TO DO] (This was done using the current qDF to set the fitting range. Nvelocity=24 and Nsigma=5 is not high enough for the largest differences, i.e. grid search and MCMC converge to different values. Redo with fiducial qDF. [TO DO] [TO DO: Add in plot a label, that it is a 50%/50% mix of a hot and a cold population.??])

3. Questions that haven't been covered so far:

- What limits the overall code speed?
- What happens, when the errors are not uniform?
- What if errors in distance matter for selection?
- Deviations from axisymmetry: Take numerical simulations.

[TO DO: Check if all references are actually used in paper. ???]

REFERENCES

[TO DO]

Binney, J. J., & McMillan, P. 2011, MNRAS, 413, 1889

Binney, J. J. 2012, MNRAS, 426, 1324

Bovy, J., Rix, H.-W., & Hogg, D. W. 2012b, ApJ, 751, 131

Bovy, J., Rix, H.-W., Hogg, D. W. et al., 2012c, ApJ, 755,115

Bovy, J., Rix, H.-W., Liu, C. et al., 2012d, ApJ, 753, 148

Bovy, J., & Rix, H.-W. 2003, ApJ, 779, 115

Piffl, T., Binney, J., & McMillan, P. J. et al., 2014, MNRAS, 455, 3133

Steinmetz, M. et al., 2006, AJ, 132, 1645

Ting, Y.-S., Rix, H.-W., Bovy, J., & van de Ven, G. 2013, MNRAS, 434, 652

Binney, J., & Tremaine, S. 2008, [TO DO: Galactic Dynamics???]

[TO DO] Extended distribution functions for our Galaxy
